

# MUSES: 3D-Controllable Image Generation via Multi-Modal Agent Collaboration

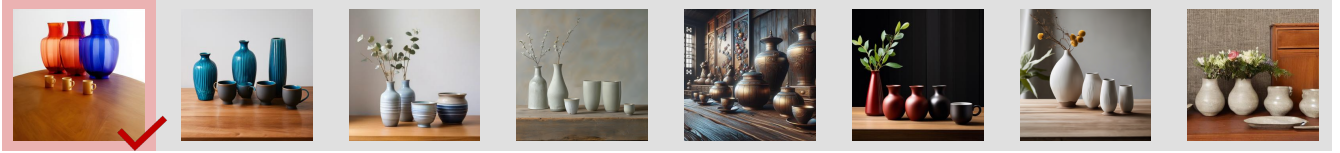
Yanbo Ding<sup>1, 2, \*</sup>, Shaobin Zhuang<sup>3, 4</sup>, Kunchang Li<sup>1, 2, 3</sup>,  
Zhengrong Yue<sup>3, 4</sup>, Yu Qiao<sup>1, 3</sup>, Yali Wang<sup>1, 3, †</sup>

<sup>1</sup>Shenzhen Institute of Advanced Technology, Chinese Academy of Sciences

<sup>2</sup>University of Chinese Academy of Sciences <sup>3</sup>Shanghai AI Laboratory <sup>4</sup>Shanghai Jiao Tong University

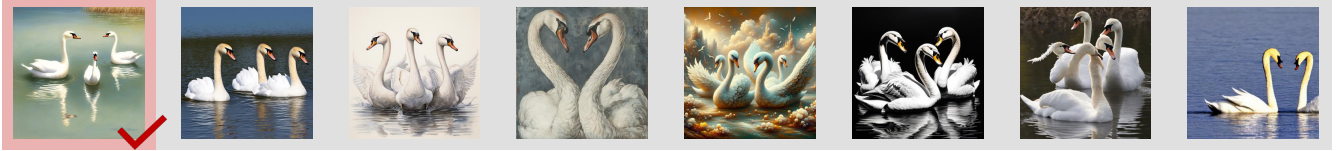
(a) Prompt containing *multiple objects*, *3D spatial relationships*, and *camera view*:

Three vases in the back and three cups in the front, evenly spaced on wooden table, right view.



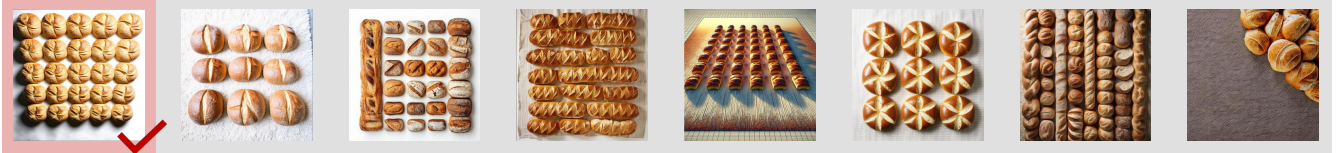
(b) Prompt containing *multiple objects*, *3D spatial relationships*, and *orientations*:

Three swans, one on the left facing right, one in the middle facing forward, one on the right facing left.



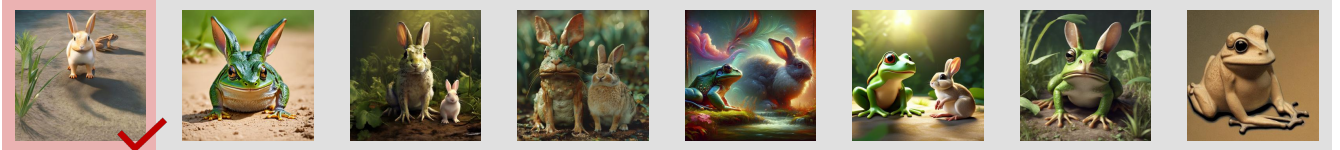
(c) Prompt containing *multiple objects*, *3D spatial relationships*, and *camera view*:

Twenty five bread arranged in five horizontal lines, fill the entire picture, on white carpet, top view.



(d) Prompt containing *3D spatial relationships*, *orientations*, and *camera view*:

A frog facing right is behind a rabbit facing forward on the ground, front view, photorealistic.



MUSES (Ours)

SD 3

Playground 2.5

Midjourney v6

DALLE3

Hunyuan-DiT

RPG-Diffusion

Structured Diffusion

Figure 1: **Comparison Results With Various Methods.** Our MUSES achieves the best, with object numbers highlighted in brown, object orientations in yellow, 3D spatial relationships in blue, and camera views in green, outperforming both open-sourced state-of-the-art methods and commercial API products, such as Stable Diffusion V3, DALL-E 3, and Midjourney v6.0.

## Abstract

Despite recent advancements in text-to-image generation, most existing methods struggle to create images with multiple objects and complex spatial relationships in 3D world. To tackle this limitation, we introduce a generic AI system, namely **MUSES**, for 3D-controllable image generation from user queries. Specifically, our MUSES addresses this challenging task by developing a progressive workflow with three key components, including (1) Layout Manager for 2D-to-3D layout lifting, (2) Model Engineer for 3D object acquisition and calibration, (3) Image Artist for 3D-to-2D image rendering.

By mimicking the collaboration of human professionals, this multi-modal agent pipeline facilitates the effective and automatic creation of images with 3D-controllable objects, through an explainable integration of top-down planning and bottom-up generation. Additionally, we find that existing benchmarks lack detailed descriptions of complex 3D spatial relationships of multiple objects. To fill this gap, we further construct a new benchmark of T2I-3DisBench (3D image scene), which describes diverse 3D image scenes with 50 detailed prompts. Extensive experiments show the state-

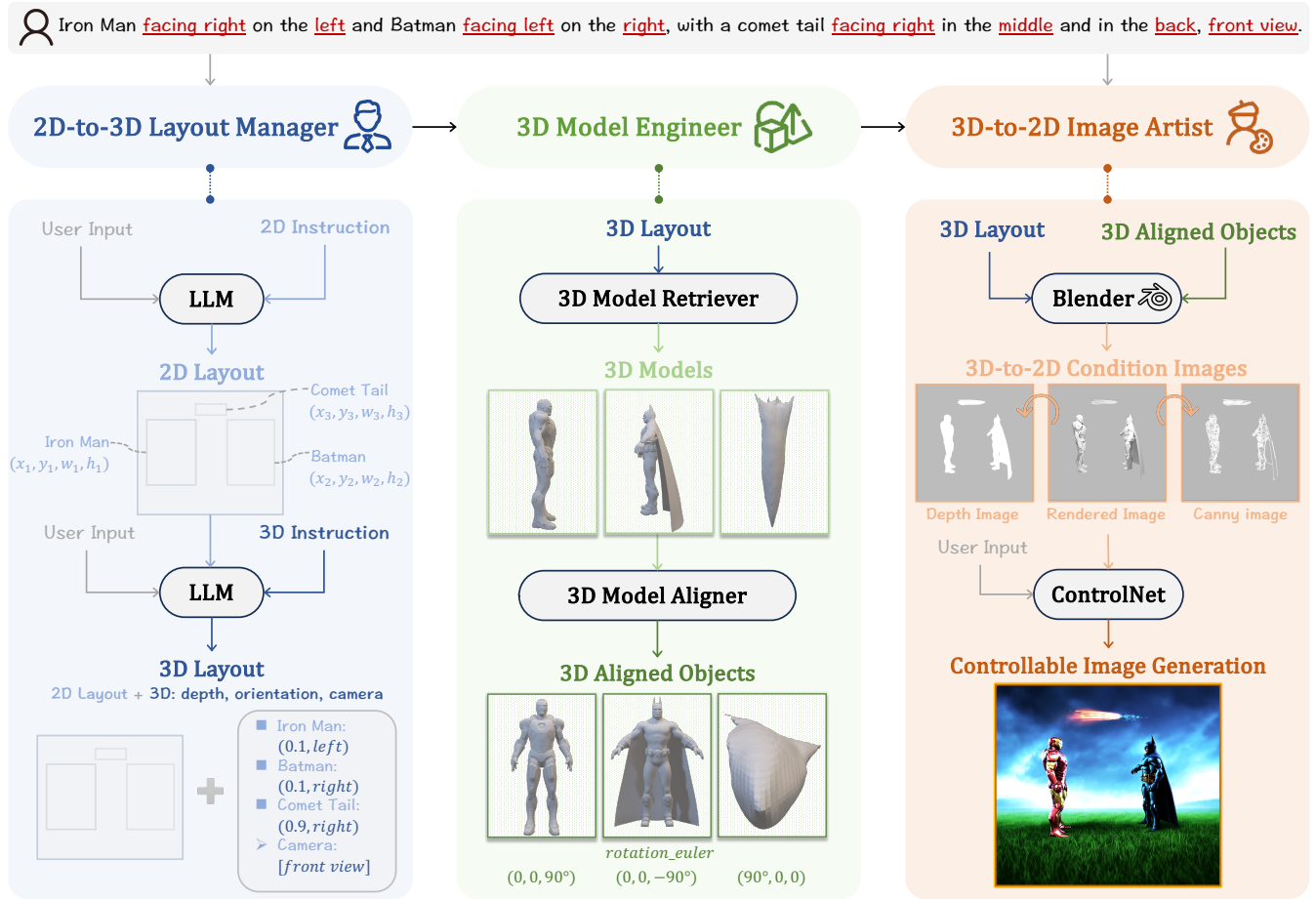


Figure 2: **Overview of our MUSES.** Based on the user input, Layout Manager first plans a 2D layout and lift it to a 3D one. Then, Model Engineer acquires 3D models of query objects and aligns them to face the camera. Finally, Image Artist assembles all the objects into visual conditions that are used for final image generation.

of-the-art performance of MUSES on both T2I-CompBench and T2I-3DisBench, outperforming recent strong competitors such as DALL-E 3 and Stable Diffusion 3. These results demonstrate a significant step of MUSES forward in bridging natural language, 2D image generation, and 3D world.

## Introduction

In recent years, we have witnessed rapid advancements in text-to-image generation (Rombach et al. 2022a; Ramesh et al. 2021; Midjourney 2024). However, such generation often struggles with detailed user queries with multiple objects in complex scenes. Several approaches have emerged to address this by compositional text-to-image synthesis (Yang et al. 2024b; Chefer et al. 2023; Feng et al. 2024; Wang et al. 2024; Feng et al. 2023; Li et al. 2023b). Unfortunately, they fail to accurately control 3D contents in the image such as 3D spatial relationship, object orientation, and camera view, even though our real world is inherently three-dimensional. As shown in Fig. 1, when the prompt is “a frog facing right is behind a rabbit facing forward on the ground”, existing approaches collapse with unsatisfactory 3D arrangement. This raises a fundamental question: can we create images with precise 3D control to better simulate our world?

To answer this question, we draw an inspiration from the workflow of 3D professionals. We observe that creating such images typically involves three key stages: scene layout planning, 3D objects design, and image rendering (Pharr, Jakob, and Humphreys 2023). This highlights the need for developing a systematic framework of 3D-controllable image creation, rather than relying on a single generation model. Therefore, we propose a generic AI system which automatically and precisely creates images with 3D controllable objects. We name it **MUSES**, since we consider human designers as our “Muses”, and mimic their workflows through a collaborative pipeline of multi-modal agents.

Our **MUSES** system, as depicted in Fig. 2, comprises three key agents that progressively achieve 3D-controllable image generation: (1) *Layout Manager*. First, we employ a Large Language Model (e.g., Llama3 (AI@Meta 2024)) as layout manager to assign 3D object locations based on user queries. Our innovative 2D-to-3D layout lifting paradigm first generates a 2D layout through in-context learning, then elevates it to a 3D layout via chain-of-thought reasoning. (2) *Model Engineer*. After obtaining the 3D layout, we introduce a model engineer to acquire 3D models of queried objects. To enhance its robustness, we design a flexible re-

triever that gathers 3D models through a decision tree approach, combining self-collected model shop retrieval, on-line search, and text-to-3D generation. Furthermore, to ensure orientation alignment with the planned 3D layout, we develop a novel aligner to calibrate object orientation by face-camera-view identification with CLIP (Radford et al. 2021). (3) *Image Artist*. Finally, we introduce an image artist to render 3D-controllable images. The 3D-aligned objects and their layouts are fed into Blender (Community 2018), which accurately assembles all the objects into 3D-to-2D condition images such as depth and canny maps. These conditions are then used with ControlNet (Zhang, Rao, and Agrawala 2023) to generate the final image of user query.

Our contributions are threefold. *First*, our MUSES is a pioneering AI system for 3D-controllable image generation, to our best knowledge. It enables precise control over object properties such as object count, orientation, 3D spatial relationships, and camera view, potentially bridging the gap between image generation and world simulation. *Second*, MUSES is a distinct multi-agent collaboration for 3D-controllable image generation. Instead of simple model invocation, each agent of MUSES is an insightful and novel integration of multi-modal agents, allowing for top-down planning and bottom-up generation with robust control of 3D information. *Finally*, since existing benchmarks lack detailed descriptions of complex 3D information like object orientation and camera view, we further construct a new benchmark of T2I-3DisBench (3D image scene), which consists of 50 prompts involving multiple objects with diverse object orientations, 3D spatial relationships, and camera views across various complex 3D scenes. Extensive experiments demonstrate the superiority of MUSES on both T2I-CompBench and our T2I-3DisBench, where it consistently outperforms state-of-the-art competitors of both open-source models and commercial API products, including Stable Diffusion v3 (Esser et al. 2024), DALL-E 3 (Betker et al. 2023) and Midjourney v6.0 (Midjourney 2024), in terms of precise 3D control in image generation.

## Related Work

**Controllable Image Generation.** Prior to diffusion models, GAN-based (Creswell et al. 2018) methods such as ControlGAN (Lee and Seok 2019) and AttnGAN (Fang et al. 2022), incorporated text features via attention (Vaswani et al. 2017) modules to guide image generation. With the advent of diffusion models (Ho, Jain, and Abbeel 2020; Sohl-Dickstein et al. 2015), Stable Diffusion series (Podell et al. 2023; Rombach et al. 2022b,a) rapidly dominated the text-to-image generation market. Given that text-based control is insufficient for precise and fine-grained image generation, ControlNet (Zhang, Rao, and Agrawala 2023), GLIGEN (Li et al. 2023b), T2I-Adapter (Mou et al. 2023) introduced additional control conditions such as depth maps and sketches. Additionally, models such as Structured-Diffusion (Feng et al. 2023) and Attn-Exct (Chefer et al. 2023) fused linguistic structures or attention-based semantic guidance into the diffusion process. Methods like VPGen (Cho, Zala, and Bansal 2024), LayoutGPT (Feng et al. 2024) and LMD (Lian et al. 2023) employed LLMs to plan 2D layouts (bounding boxes),

while RPG (Yang et al. 2024b) used LLMs to plan and assign regions, and to re-caption the user input. Despite these advancements, existing methods struggle to control 3D properties of objects. We take an innovative approach by planning 3D layouts and incorporating 3D models and simulation to achieve 3D controllable image generation.

**LLM-Based Agents.** LLMs such as ChatGPT (Brown et al. 2020; Achiam et al. 2023), Llama (Touvron et al. 2023a,b) have revolutionized natural language processing, while Multimodal LLMs (MLLMs) such as LLaVA (Liu et al. 2024), InternVL (Chen et al. 2024b) have enabled impressive performance on visual tasks. The combination of LLMs and MLLMs in multi-agent systems has achieved remarkable success across various domains, including visual understanding (Kelly et al. 2024; Wu et al. 2023a), gaming (Li et al. 2023a; Gong et al. 2023), software development (Wu et al. 2023b; Qian et al. 2023), video generation (Yuan et al. 2024; Yang et al. 2024a), and autonomous driving (Wei et al. 2024; Palanisamy 2020). We focus on image generation via multi-agent collaboration. DiffusionGPT (Qin et al. 2024) employed LLMs for model selection in image generation. SLD (Wu et al. 2024) used LLMs for self-correction of the generated image. CompAgent (Wang et al. 2024) leveraged LLMs to coordinate and plan the image generation process into sub-steps. Unlike these works, we use LLMs to plan 3D layouts, bridging the gap between linguistic understanding and 3D spatial reasoning, particularly in complex 3D scenes.

## Method

In this section, we introduce our MUSES for 3D controllable image generation. As shown in Fig. 2, it is a generic AI system with distinct multi-modal agent collaboration pipeline. Specifically, our MUSES consists of three collaborative agents including Layout Manager for 2D-to-3D layout lifting, Model Engineer for 3D object acquisition and calibration, Image Artist for 3D-to-2D image rendering.

### Lifting: 2D-to-3D Layout Manager

To achieve precise 3D control, we first plan 3D layout according to the user input. Specifically, we employ LLM (e.g., Llama3 (AI@Meta 2024)) as a layout manager, due to its great power of linguistic understanding. To alleviate planning difficulty, we design a 2D-to-3D lifting paradigm for progressive transition from 2D to 3D layout in Fig. 3.

**2D Layout Planning via In-Context-Learning.** We start with 2D layout planning to determine the 2D location of objects. Apparently, asking the LLM directly to generate an object layout is not ideal, as it may struggle with managing bounding boxes in images. Hence, we leverage In-Context Learning (Dong et al. 2022), allowing the LLM to follow instructions with a few examples from a 2D layout shop. We use the NSR-1K dataset (Feng et al. 2024) as the 2D layout shop, since it contains over 40,000 entries with diverse prompts, objects, and the corresponding bounding boxes. First, we use the CLIP (Radford et al. 2021) text encoder to compare similarities of user input and text prompts in the shop. Then, we select the top five 2D layouts with the highest similarity scores. Finally, we feed these contextual lay-

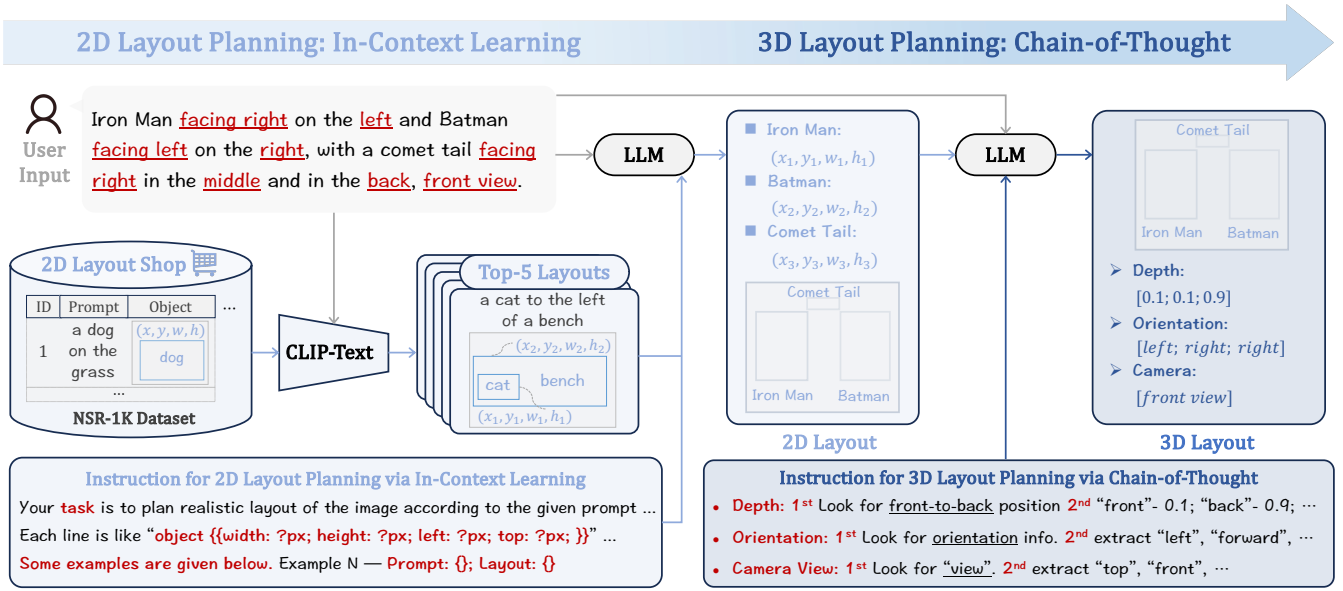


Figure 3: **2D-to-3D Layout Manager.** First, based on the user input, our layout manager employs the LLM to plan 2D layout through In-context Learning. Then, it lifts 2D layout to 3D space via Chain of Thought reasoning.

outs along with instructions to the LLM, guiding it to generate a 2D layout of the user input. Such a comprehensive approach results in a contextually-relevant 2D layout, forming the foundation for the subsequent 3D lifting.

**3D Layout Planning via Chain-of-Thought.** Unlike the previous approaches (Feng et al. 2024; Qu et al. 2023; Cho, Zala, and Bansal 2024; Lian et al. 2023) that directly perform transition from 2D layout to image generation, we lift our 2D layout to 3D space. Specifically, guided by the 2D layout and user input, we further ask the LLM to determine 3D attributes, including object depth, orientation and camera view. To enhance complex planning capability, we design a chain-of-thought (CoT) prompting (Wei et al. 2022) for step-by-step reasoning on each attribute. Taking object depth as an example, the first-step instruction is to look for the front-to-back position relationships in the user input. Based on such relationships, the second-step instruction is to assign the depth value to each object, (e.g., "A is in front of B": depth of A is set as 0.1 and depth of B is set as 0.9 which will be used in Blender later). The instructions for object orientation and camera view are similar. We list all the instructions in Supplementary Material Section A. Via such a manager, we are able to accurately exploit 3D layout in the user input for subsequent 3D simulation.

### Calibrating: 3D Model Engineer

After planning 3D layout of user input, the next step is to find 3D models of the specified objects. To achieve this, we introduce a 3D Model Engineer which comprises two key roles: Model Retriever for acquiring 3D models of objects according to the 3D layout, Model Aligner for calibrating the orientations of acquired 3D models to face the camera.

**3D Model Retriever: Retrieve-Generate Decision Tree.** To obtain 3D object models with efficiency and robustness, we design a concise Model Retriever via the decision tree

of retrieval and generation in Fig. 4. Our motivation is that, 3D object models from internet often exhibit richer diversity and higher fidelity, compared to those generated by text-to-3D synthesis. Hence, we prioritize the retrieval of existing 3D models in the decision tree, which not only enhances the overall visual quality of 3D models, but also reduces computational load in text-to-3D synthesis.

Specifically, our model retriever is based on a self-collected 3D model shop (300 3D models of 230 object categories) that is built in an online fashion. *First*, this model retriever looks for 3D models of queried objects from the current shop, using the object name as the search key. *Second*, if it does not find any 3D models of a queried object from this shop (e.g., Batman in Fig. 4), it will search them online, e.g., on the professional website (<https://www.cgtrader.com>). For each object, there may exist a number of 3D models from such a web. Hence, we performs CLIP text encoder to calculate similarity between object name and online item title, and select the 3D model with the highest similarity. *Third*, if all the online search fails in finding 3D models of queried objects (e.g., Comet Halley in Fig. 4), then we will employ a text-to-3D generation model like Shap-E (Jun and Nichol 2023) or 3DTopia (Hong et al. 2024) to synthesize the corresponding 3D model. *Finally*, we put the newly-found object models into 3D shop for enhancing shop diversity and versatility of future usage. Via such a model retriever, we can quickly obtain appropriate 3D models of query objects and remains up-to-date with the latest available high-quality models, ensuring both efficiency and robustness.

**3D Model Aligner: Face-Camera Calibration.** As 3D models are acquired from internet or generation, their orientations may not align with the expected ones in the planned 3D layout. To address this, we introduce a novel 3D Model Aligner, which can calibrate the original orientation of 3D object models to face camera, for further usage along with



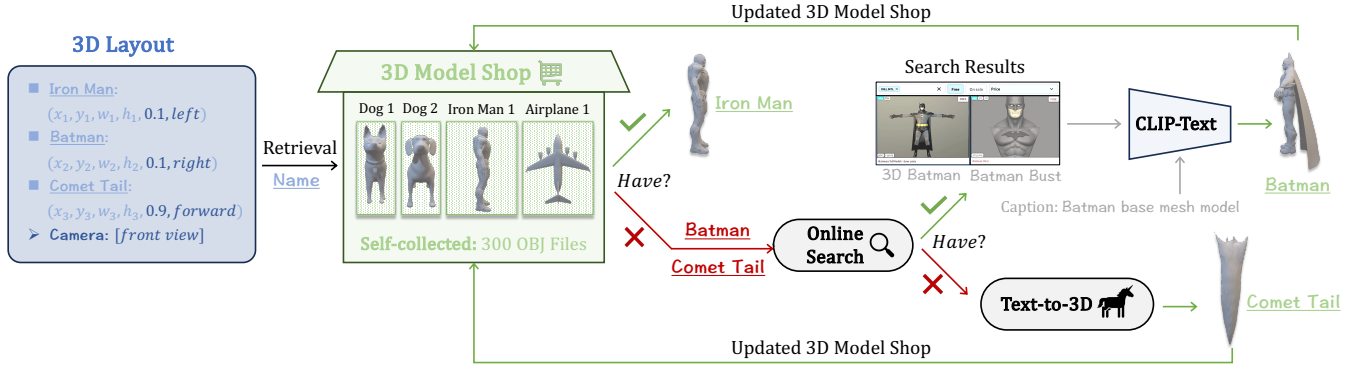


Figure 4: **3D Model Retriever.** We develop a retrieve-generate decision tree that automatically acquires 3D objects specified in the 3D layout from a self-collected model shop, based on a concise decision process of online search and text-to-3D generation.

3D layout later. To achieve this goal, it basically fine-tunes the CLIP as a face-camera classifier, as shown in Fig. 5.

*Fine-tuning CLIP as a Face-Camera Classifier.* First, we prepare the training dataset for fine-tuning. Specifically, we randomly select 150 3D models from our 3D shop, and feed them into Blender with a standardized environment. For each 3D model, we perform multi-view rendering to generate a set of 2D images from various views, under different rotation\_euler parameters in Blender. Subsequently, we annotate each image by tagging the description of “object name (faces / not face) camera”. To increase data diversity across diverse 3D geometries, we randomly select 5 no-face-camera images as negative samples for each 3D model. To balance positive and negative samples during fine-tuning, we make the face-camera image as 5 copies for each 3D model. This results in a training set with 1500 image-text pairs, which are used for fine-tuning CLIP as a Face-Camera Classifier by contrastive language-image learning.

*Inferring Face-Camera Image of 3D Object Models.* During inference, we import 3D models of queried objects (from model retriever) into the same Blender environment used in training dataset generation. For each 3D model, we also perform multi-view rendering to generate a comprehensive set of 2D images from various views. Then, we use the fine-tuned CLIP to identify the face-camera image of each 3D model, by comparing similarity between the rendered images and the text “object name faces camera”. Based on this image, we can effectively align 3D object models to face camera through the configuration of the rotation parameter in Blender, which is used to generate correctly-orientated objects in the subsequent 3D-to-2D image generation.

### Rendering: 3D-to-2D Image Artist

So far, we have obtained 3D layout and aligned 3D models of objects from the user query. Given these 3D materials, we next introduce a concise image artist that can generate the 3D-controllable image, based on a 3D-to-2D condition rendering as shown in Fig. 2. First, we assemble all the 3D object models into a complete scene, according to the 3D layout. To ensure consistent and accurate 3D scene composition, we develop a comprehensive setting of parameter configuration in Blender, including settings of global environment, rendering, camera, light, and object. Our imple-

mentation details in Blender are provided in Supplementary Material Section C. Once the 3D scene is fully assembled, we use Blender’s rendering engine (e.g. “CYCLES” Rendering Engine) to convert the 3D scene into a high-quality 2D image, which accurately captures position, size, and orientation of objects represented as simplified geometric shapes. To further enhance the control over the final image generation, we process this 2D rendering into two condition images, including the (1) Depth Map by Blender’s Z-pass rendering (Ouza, Ulrich, and Yang 2017), representing 3D spatial relationships. (2) Canny Edge Image by OpenCV (Bradski 2000), highlighting object contours. Finally, we leverage these 3D-to-2D condition images as fine-grained control, and employ advanced image generation techniques such as ControlNet (Zhang, Rao, and Agrawala 2023), to generate the final image with accuracy from the user input. Via such a concise image artist, our MUSES can flexibly generate a 3D-controllable image that accurately reflects both 3D spatial details and semantic contents of the user input.

## Experiment

**Datasets and Metrics.** We first conducted experiments on T2I-CompBench (Huang et al. 2023) due to its comprehensive evaluations of object count and spatial relationships. However, T2I-CompBench lacks detailed text prompts of object orientations and camera views. To fill this gap, we further introduce T2I-3DisBench (3D image scene), a dataset of 50 detailed texts that encapsulate complex 3D information (details provided in Supplementary Material Section B). We conducted both automatic and user evaluations on our T2I-3DisBench. Since the metrics of T2I-compBench are inadequate for assessing these more detailed 3D features, we uniquely employed Visual Question Answering (VQA) on InternVL (Chen et al. 2024b). Specifically, we fed instructions (shown in Supplementary Material Section B) to InternVL, asking it to rate the generated images considering four key dimensions: object count, orientation, 3D spatial relationship, and camera view. Additionally, we conducted user evaluation on our T2I-3DisBench, where participants rate the images based on the same four dimensions.

**Implementation Details.** Our MUSES is designed to be modular and extensible, allowing for the integration of various LLMs, CLIPs and ControlNets. In our experimental

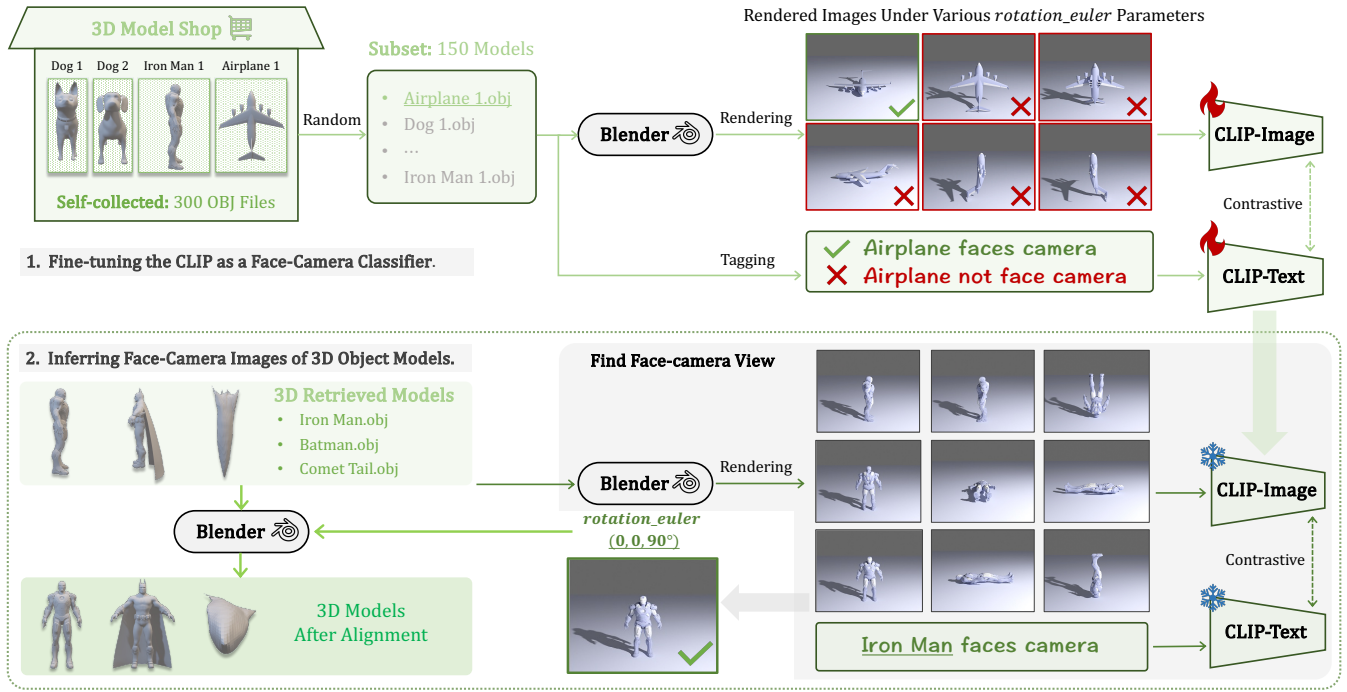


Figure 5: **3D Model Aligner**. It aligns 3D object models with face-camera orientation, ensuring that the final orientation conforms to the 3D layout. First, we fine-tune the CLIP as a Face-Camera Classifier, by a training set generated from our 3D shop. Then, we use the fine-tuned CLIP to identify face-camera image of each queried object, aligning its 3D model to face camera.

setup, we employed Llama-3-8B (AI@Meta 2024) for 3D layout planning, ViT-L/14 for image and text encoding, ViT-B/32 for orientation calibration, and SD 3 ControlNet (Zhang, Rao, and Agrawala 2023) for 3D controllable image generation. For Llama-3-8B, we set top\_p to 0.1 and temperature to 0.2 to ensure precise, consistent, and reliable outputs. For SD 3 ControlNet, we set inference step to 20 and control scale to 0.5, as discussed in parameter ablation in Supplementary Material Section D. The Blender’s parameter conversion rules and settings are also specified in Supplementary Material Section C. Additionally, we employed Mini-InternVL 1.5 (Chen et al. 2024a) for automated evaluation on T2I-3DisBench (implementation details in Supplementary Material). All experiments are conducted on Ubuntu 20.04 system with 8 NVIDIA RTX 3090 GPUs.

**SOTA Comparison on T2I-Compbench.** As shown in Tab. 1, we compared our MUSES with two types of existing SOTA methods: specialized/multi-agent approaches in the upper part and generic models in the lower part. MUSES consistently outperforms both categories across all metrics, including object count, relationship, and attribute binding. Specifically, Our innovative 3D layout planning and 3D-to-2D image conditions enhance object relationship understanding, leading to best performance on spatial-related metrics. Additionally, precise object positioning boosts the numeracy score, and detailed 3D model shape guidance significantly improves attribute binding scores.

**SOTA Comparison on T2I-3DisBench.** As shown in Tab. 2, we conducted both automatic and user evaluations (in parentheses) on our T2I-3DisBench and compared two types of SOTA methods as well. *For automatic evaluation on*

*InternVL-VQA metrics*, our MUSES consistently outperforms others, including the open-source SOTA model, Stable Diffusion V3, and closed-source API products like Mid-journey v6.0. Obviously, existing approaches struggle with complex prompts containing 3D information (e.g., object orientation, camera view), highlighting the importance of our 3D-integration design. *For user evaluation*, We randomly selected 20 prompts from our T2I-3DisBench and engaged 30 participants to rate image accuracy on a scale of 0.0 (poor) to 1.0 (excellent) across four dimensions. The results show a strong preference for MUSES, demonstrating its effectiveness in handling complex 3D scenes.

**Ablation Studies of Different Components.** As shown in Table 3, our full system achieves the best performance, and removing any component degrades the results. (1) *Object Depth Planning* is essential, as its removal leads to poor 3D spatial representation in Blender, affecting both datasets. (2) *Object Orientation Planning* is critical for prompts containing orientation information, with a score dropping on T2I-3DisBench when removed. (3) *Camera View Planning* also affects performance on T2I-3DisBench, since it contains camera information. (4) *Retrieve-Generate Decision Tree* significantly influences performance on both datasets, highlighting the importance of high-quality 3D models. (5) *Face-Camera Calibration* is the most important; its removal causes sharp performance drops as models lose correct orientation in the 3D layout. (6) *CLIP Fine-tuning During Calibration* improves CLIP’s accuracy in determining object orientations, thus enhancing the orientation accuracy of our final image. (7) *Co-ablation of Multiple Components* (last four columns) shows that removing the Model Engineer has

Method	Attribute Binding			Object Relationship			Numeracy $\uparrow$
	Color $\uparrow$	Shape $\uparrow$	Texture $\uparrow$	2D-Spatial $\uparrow$	3D-Spatial $\uparrow$	Non-Spatial $\uparrow$	
LayoutGPT (Feng et al. 2024)	0.2921	0.3716	0.3310	0.1153	0.2607	0.2989	0.4193
Structured Diffusion (Feng et al. 2023)	0.4990	0.4218	0.4900	0.1386	0.2952	0.3111	0.4562
Attn-Exct (Chefer et al. 2023)	0.6400	0.4517	0.5963	0.1455	-	0.3109	-
GORS (Huang et al. 2023)	0.6603	0.4785	0.6287	0.1815	-	0.3193	-
RPG-Diffusion (Yang et al. 2024b)	0.6024	0.4597	0.5326	0.2115	0.3587	0.3104	0.4968
CompAgent (Wang et al. 2024)	0.6994	0.5740	0.6927	0.3138	-	0.3102	-
SD v1.4 (Rombach et al. 2022a)	0.3765	0.3576	0.4156	0.1350	0.3336	0.3079	0.4418
SD v2 (Rombach et al. 2022b)	0.5065	0.4221	0.4922	0.1703	0.3205	0.3096	0.4849
SDXL (Podell et al. 2023)	0.6369	0.5408	0.5637	0.2032	0.3438	0.3110	0.5145
PixArt- $\alpha$ (Chen et al. 2023)	0.6886	0.5582	0.7044	0.2082	0.3530	0.3179	0.5001
Playground v2.5 (Li et al. 2024a)	0.6381	0.4790	0.6297	0.2062	0.3816	0.3108	0.5329
Hunyuan-DiT (Li et al. 2024b)	0.6342	0.4641	0.5328	0.2337	0.3731	0.3063	0.5153
<b>MUSES(Ours)</b>	<b>0.7668</b>	<b>0.5762</b>	<b>0.7206</b>	<b>0.3544</b>	<b>0.3893</b>	<b>0.3214</b>	<b>0.5673</b>

Table 1: **Evaluation Results on T2I-CompBench.** Our MUSES demonstrates the best performance on attribute binding, object relationship, and object count, outperforming SOTA methods, including multi-agent specialized methods, and generic models.

Method	Average Score $\uparrow$	Object Count $\uparrow$	Orientation $\uparrow$	3D Spatial Relationship $\uparrow$	Camera View $\uparrow$
Structured Diffusion (Feng et al. 2023)	0.2202 (0.15)	0.2308 (0.14)	0.1770 (0.08)	0.3040 (0.21)	0.1690 (0.18)
RPG-Diffusion (Yang et al. 2024b)	0.2444 (0.18)	0.3100 (0.18)	0.2275 (0.15)	0.2295 (0.25)	0.2105 (0.12)
LayoutGPT (Feng et al. 2024)	0.2957 (0.14)	0.3246 (0.14)	0.1659 (0.12)	0.4587 (0.18)	0.2337 (0.10)
Playground v2.5 (Li et al. 2024a)	0.1776 (0.19)	0.2300 (0.19)	0.1502 (0.17)	0.2050 (0.28)	0.1250 (0.15)
DALL-E 3 (Betker et al. 2023)	0.1925 (0.23)	0.1960 (0.15)	0.1720 (0.18)	0.2027 (0.29)	0.1990 (0.29)
Hunyuan-DiT (Li et al. 2024b)	0.2099 (0.22)	0.2130 (0.19)	0.1780 (0.21)	0.2509 (0.29)	0.1975 (0.18)
Midjourney v6.0 (Midjourney 2024)	0.3538 (0.35)	0.3820 (0.39)	0.3322 (0.27)	0.3880 (0.36)	0.3130 (0.38)
Stable Diffusion V3 (Esser et al. 2024)	0.4443 (0.36)	0.5840 (0.42)	0.3590 (0.26)	0.5081 (0.40)	0.3260 (0.33)
<b>MUSES(Ours)</b>	<b>0.5192 (0.62)</b>	<b>0.6180 (0.61)</b>	<b>0.4610 (0.68)</b>	<b>0.5647 (0.62)</b>	<b>0.4330 (0.57)</b>

Table 2: **Evaluation Results on our T2I-3DisBench.** Our MUSES consistently outperforms other methods across all metrics. Each cell displays both the InternVL-VQA metric value and the corresponding score from user evaluation (in parentheses).

Component	Choice											
Object Depth Planning	✓	✗	✓	✓	✓	✓	✓	✗	✓	✗	✗	✗
Object Orientation Planning	✓	✓	✗	✓	✓	✓	✓	✗	✓	✗	✗	✗
Camera View Planning	✓	✓	✓	✗	✓	✓	✓	✗	✓	✗	✗	✗
Retrieve-Generate Decision Tree	✓	✓	✓	✓	✓	✗	✓	✓	✗	✗	✓	✓
Face-Camera Calibration	✓	✓	✓	✓	✗	✓	✓	✓	✗	✓	✗	✗
CLIP Fine-tuning During Calibration	✓	✓	✓	✓	✗	✓	✗	✓	✗	✓	✗	✗
Results on T2I-CompBench	<b>0.3893</b>	0.3647	0.3816	0.3893	0.3536	0.3567	0.3640	0.3517	0.3439	0.3471	0.3406	
Results on T2I-3DisBench	<b>0.5192</b>	0.3852	0.4025	0.4580	0.3837	0.4988	0.4437	0.3455	0.3558	0.3301	0.2980	

Table 3: **Ablation Studies of Different Components on T2I-CompBench and on our T2I-3DisBench.** Where T2I-CompBench uses the 3D-spatial metric because it is most relevant to the 3D environment, and T2I-3DisBench uses the average InternVL-VQA score in terms of object count, object orientation, 3D spatial relationship and camera view.

the most significant impact, resulting in poor object shaping and orientation. Removing the Layout Manager also notably degrades performance. These findings demonstrate the interconnected nature of our system’s components and their effects on overall performance, with each component being crucial for 3D controllable image generation.

## Conclusion

We introduce MUSES, a multi-agent collaborative system for precise 3D controllable image generation. By integrating 3D layouts, models and simulation, MUSES achieves fine-grained control over 3D object properties (e.g. object orientation, 3D spatial relationship) and camera view. To evalu-

ate such complex 3D image scenes more comprehensively, we construct a new benchmark named T2I-3DisBench. Experiments on T2I-CompBench and our new T2I-3DisBench demonstrate superior performance of MUSES in handling complex 3D scenes. Future work will focus on improving efficiency and expanding capabilities to control lighting conditions, and potentially expanding to video generation.

## Acknowledgments

We acknowledge the contributions of teams at OpenAI, Meta AI, and InstantX for their open-source models, and CGTrader for supporting 3D model crawler free downloads. We appreciate as well the valuable insights from researchers at the Shenzhen Institute of Advanced Technology and the Shanghai AI Laboratory.

## References

- Achiam, J.; Adler, S.; Agarwal, S.; Ahmad, L.; Akkaya, I.; Aleman, F. L.; Almeida, D.; Altenschmidt, J.; Altman, S.; Anadkat, S.; et al. 2023. Gpt-4 technical report. *arXiv preprint arXiv:2303.08774*.
- AI@Meta. 2024. Llama 3 Model Card.
- Betker, J.; Goh, G.; Jing, L.; Brooks, T.; Wang, J.; Li, L.; Ouyang, L.; Zhuang, J.; Lee, J.; Guo, Y.; et al. 2023. Improving image generation with better captions. *Computer Science*. <https://cdn.openai.com/papers/dall-e-3.pdf>, 2(3): 8.
- Bradski, G. 2000. The OpenCV Library. *Dr. Dobb's Journal of Software Tools*.
- Brown, T.; Mann, B.; Ryder, N.; Subbiah, M.; Kaplan, J. D.; Dhariwal, P.; Neelakantan, A.; Shyam, P.; Sastry, G.; Askell, A.; et al. 2020. Language models are few-shot learners. *Advances in neural information processing systems*, 33: 1877–1901.
- Chefer, H.; Alaluf, Y.; Vinker, Y.; Wolf, L.; and Cohen-Or, D. 2023. Attend-and-excite: Attention-based semantic guidance for text-to-image diffusion models. *ACM Transactions on Graphics (TOG)*, 42(4): 1–10.
- Chen, J.; Yu, J.; Ge, C.; Yao, L.; Xie, E.; Wu, Y.; Wang, Z.; Kwok, J.; Luo, P.; Lu, H.; et al. 2023. Pixart- $\alpha$ : Fast training of diffusion transformer for photorealistic text-to-image synthesis. *arXiv preprint arXiv:2310.00426*.
- Chen, Z.; Wang, W.; Tian, H.; Ye, S.; Gao, Z.; Cui, E.; Tong, W.; Hu, K.; Luo, J.; Ma, Z.; et al. 2024a. How Far Are We to GPT-4V? Closing the Gap to Commercial Multimodal Models with Open-Source Suites. *arXiv preprint arXiv:2404.16821*.
- Chen, Z.; Wu, J.; Wang, W.; Su, W.; Chen, G.; Xing, S.; Zhong, M.; Zhang, Q.; Zhu, X.; Lu, L.; et al. 2024b. Internvl: Scaling up vision foundation models and aligning for generic visual-linguistic tasks. In *Proceedings of the IEEE/CVF Conference on Computer Vision and Pattern Recognition*, 24185–24198.
- Cho, J.; Zala, A.; and Bansal, M. 2024. Visual programming for step-by-step text-to-image generation and evaluation. *Advances in Neural Information Processing Systems*, 36.
- Community, B. O. 2018. *Blender - a 3D modelling and rendering package*. Blender Foundation, Stichting Blender Foundation, Amsterdam.
- Creswell, A.; White, T.; Dumoulin, V.; Arulkumaran, K.; Sengupta, B.; and Bharath, A. A. 2018. Generative adversarial networks: An overview. *IEEE signal processing magazine*, 35(1): 53–65.
- Dong, Q.; Li, L.; Dai, D.; Zheng, C.; Wu, Z.; Chang, B.; Sun, X.; Xu, J.; and Sui, Z. 2022. A survey on in-context learning. *arXiv preprint arXiv:2301.00234*.
- Esser, P.; Kulal, S.; Blattmann, A.; Entezari, R.; Müller, J.; Saini, H.; Levi, Y.; Lorenz, D.; Sauer, A.; Boesel, F.; et al. 2024. Scaling rectified flow transformers for high-resolution image synthesis. In *Forty-first International Conference on Machine Learning*.
- Fang, F.; Zhang, P.; Zhou, B.; Qian, K.; and Gan, Y. 2022. Atten-GAN: pedestrian trajectory prediction with gan based on attention mechanism. *Cognitive Computation*, 14(6): 2296–2305.
- Feng, W.; He, X.; Fu, T.-J.; Jampani, V.; Akula, A.; Narayana, P.; Basu, S.; Wang, X. E.; and Wang, W. Y. 2023. Training-Free Structured Diffusion Guidance for Compositional Text-to-Image Synthesis. *arXiv:2212.05032*.
- Feng, W.; Zhu, W.; Fu, T.-j.; Jampani, V.; Akula, A.; He, X.; Basu, S.; Wang, X. E.; and Wang, W. Y. 2024. Lay-outgpt: Compositional visual planning and generation with large language models. *Advances in Neural Information Processing Systems*, 36.
- Gong, R.; Huang, Q.; Ma, X.; Vo, H.; Durante, Z.; Noda, Y.; Zheng, Z.; Zhu, S.-C.; Terzopoulos, D.; Fei-Fei, L.; et al. 2023. Mindagent: Emergent gaming interaction. *arXiv preprint arXiv:2309.09971*.
- Ho, J.; Jain, A.; and Abbeel, P. 2020. Denoising diffusion probabilistic models. *Advances in neural information processing systems*, 33: 6840–6851.
- Hong, F.; Tang, J.; Cao, Z.; Shi, M.; Wu, T.; Chen, Z.; Wang, T.; Pan, L.; Lin, D.; and Liu, Z. 2024. 3DTopia: Large Text-to-3D Generation Model with Hybrid Diffusion Priors. *arXiv preprint arXiv:2403.02234*.
- Huang, K.; Sun, K.; Xie, E.; Li, Z.; and Liu, X. 2023. T2i-compbench: A comprehensive benchmark for open-world compositional text-to-image generation. *Advances in Neural Information Processing Systems*, 36: 78723–78747.
- Jun, H.; and Nichol, A. 2023. Shap-e: Generating conditional 3d implicit functions. *arXiv preprint arXiv:2305.02463*.
- Kelly, C.; Hu, L.; Yang, B.; Tian, Y.; Yang, D.; Yang, C.; Huang, Z.; Li, Z.; Hu, J.; and Zou, Y. 2024. Visiongpt: Vision-language understanding agent using generalized multimodal framework. *arXiv preprint arXiv:2403.09027*.
- Lee, M.; and Seok, J. 2019. Controllable generative adversarial network. *Ieee Access*, 7: 28158–28169.
- Li, D.; Kamko, A.; Akhgari, E.; Sabet, A.; Xu, L.; and Doshi, S. 2024a. Playground v2.5: Three Insights towards Enhancing Aesthetic Quality in Text-to-Image Generation. *arXiv:2402.17245*.



- Li, H.; Chong, Y. Q.; Stepputtis, S.; Campbell, J.; Hughes, D.; Lewis, M.; and Sycara, K. 2023a. Theory of mind for multi-agent collaboration via large language models. *arXiv preprint arXiv:2310.10701*.
- Li, J.; Li, D.; Xiong, C.; and Hoi, S. 2022. Blip: Bootstrapping language-image pre-training for unified vision-language understanding and generation. In *International conference on machine learning*, 12888–12900. PMLR.
- Li, Y.; Liu, H.; Wu, Q.; Mu, F.; Yang, J.; Gao, J.; Li, C.; and Lee, Y. J. 2023b. Gligen: Open-set grounded text-to-image generation. In *Proceedings of the IEEE/CVF Conference on Computer Vision and Pattern Recognition*, 22511–22521.
- Li, Z.; Zhang, J.; Lin, Q.; Xiong, J.; Long, Y.; Deng, X.; Zhang, Y.; Liu, X.; Huang, M.; Xiao, Z.; et al. 2024b. Hunyuan-DiT: A Powerful Multi-Resolution Diffusion Transformer with Fine-Grained Chinese Understanding. *arXiv preprint arXiv:2405.08748*.
- Lian, L.; Li, B.; Yala, A.; and Darrell, T. 2023. Llm-grounded diffusion: Enhancing prompt understanding of text-to-image diffusion models with large language models. *arXiv preprint arXiv:2305.13655*.
- Liu, H.; Li, C.; Wu, Q.; and Lee, Y. J. 2024. Visual instruction tuning. *Advances in neural information processing systems*, 36.
- Midjourney. 2024. Midjourney v6.0. <https://www.midjourney.com>. Image generation AI.
- Mou, C.; Wang, X.; Xie, L.; Wu, Y.; Zhang, J.; Qi, Z.; Shan, Y.; and Qie, X. 2023. T2I-Adapter: Learning Adapters to Dig out More Controllable Ability for Text-to-Image Diffusion Models. *arXiv:2302.08453*.
- Ouza, M.; Ulrich, M.; and Yang, B. 2017. A simple radar simulation tool for 3D objects based on blender. In *2017 18th International Radar Symposium (IRS)*, 1–10. IEEE.
- Palanisamy, P. 2020. Multi-agent connected autonomous driving using deep reinforcement learning. In *2020 International Joint Conference on Neural Networks (IJCNN)*, 1–7. IEEE.
- Pharr, M.; Jakob, W.; and Humphreys, G. 2023. *Physically based rendering: From theory to implementation*. MIT Press.
- Podell, D.; English, Z.; Lacey, K.; Blattmann, A.; Dockhorn, T.; Müller, J.; Penna, J.; and Rombach, R. 2023. SDXL: Improving Latent Diffusion Models for High-Resolution Image Synthesis. *arXiv:2307.01952*.
- Qian, C.; Cong, X.; Yang, C.; Chen, W.; Su, Y.; Xu, J.; Liu, Z.; and Sun, M. 2023. Communicative agents for software development. *arXiv preprint arXiv:2307.07924*.
- Qin, J.; Wu, J.; Chen, W.; Ren, Y.; Li, H.; Wu, H.; Xiao, X.; Wang, R.; and Wen, S. 2024. Diffusiongpt: LLM-driven text-to-image generation system. *arXiv preprint arXiv:2401.10061*.
- Qu, L.; Wu, S.; Fei, H.; Nie, L.; and Chua, T.-S. 2023. Layoutllm-t2i: Eliciting layout guidance from llm for text-to-image generation. In *Proceedings of the 31st ACM International Conference on Multimedia*, 643–654.
- Radford, A.; Kim, J. W.; Hallacy, C.; Ramesh, A.; Goh, G.; Agarwal, S.; Sastry, G.; Askell, A.; Mishkin, P.; Clark, J.; et al. 2021. Learning transferable visual models from natural language supervision. In *International conference on machine learning*, 8748–8763. PMLR.
- Ramesh, A.; Pavlov, M.; Goh, G.; Gray, S.; Voss, C.; Radford, A.; Chen, M.; and Sutskever, I. 2021. Zero-shot text-to-image generation. In *International conference on machine learning*, 8821–8831. Pmlr.
- Rombach, R.; Blattmann, A.; Lorenz, D.; Esser, P.; and Ommer, B. 2022a. High-resolution image synthesis with latent diffusion models. In *Proceedings of the IEEE/CVF conference on computer vision and pattern recognition*, 10684–10695.
- Rombach, R.; Blattmann, A.; Lorenz, D.; Esser, P.; and Ommer, B. 2022b. High-Resolution Image Synthesis With Latent Diffusion Models. In *Proceedings of the IEEE/CVF Conference on Computer Vision and Pattern Recognition (CVPR)*, 10684–10695.
- Sohl-Dickstein, J.; Weiss, E.; Maheswaranathan, N.; and Ganguli, S. 2015. Deep unsupervised learning using nonequilibrium thermodynamics. In *International conference on machine learning*, 2256–2265. PMLR.
- Touvron, H.; Lavril, T.; Izacard, G.; Martinet, X.; Lachaux, M.-A.; Lacroix, T.; Rozière, B.; Goyal, N.; Hambro, E.; Azhar, F.; et al. 2023a. Llama: Open and efficient foundation language models. *arXiv preprint arXiv:2302.13971*.
- Touvron, H.; Martin, L.; Stone, K.; Albert, P.; Almahairi, A.; Babaei, Y.; Bashlykov, N.; Batra, S.; Bhargava, P.; Bhosale, S.; et al. 2023b. Llama 2: Open foundation and fine-tuned chat models. *arXiv preprint arXiv:2307.09288*.
- Vaswani, A.; Shazeer, N.; Parmar, N.; Uszkoreit, J.; Jones, L.; Gomez, A. N.; Kaiser, Ł.; and Polosukhin, I. 2017. Attention is all you need. *Advances in neural information processing systems*, 30.
- Wang, Z.; Xie, E.; Li, A.; Wang, Z.; Liu, X.; and Li, Z. 2024. Divide and Conquer: Language Models can Plan and Self-Correct for Compositional Text-to-Image Generation. *arXiv:2401.15688*.
- Wei, J.; Wang, X.; Schuurmans, D.; Bosma, M.; Xia, F.; Chi, E.; Le, Q. V.; Zhou, D.; et al. 2022. Chain-of-thought prompting elicits reasoning in large language models. *Advances in neural information processing systems*, 35: 24824–24837.
- Wei, Y.; Wang, Z.; Lu, Y.; Xu, C.; Liu, C.; Zhao, H.; Chen, S.; and Wang, Y. 2024. Editable scene simulation for autonomous driving via collaborative llm-agents. In *Proceedings of the IEEE/CVF Conference on Computer Vision and Pattern Recognition*, 15077–15087.
- Wu, C.; Yin, S.; Qi, W.; Wang, X.; Tang, Z.; and Duan, N. 2023a. Visual chatgpt: Talking, drawing and editing with visual foundation models. *arXiv preprint arXiv:2303.04671*.
- Wu, Q.; Bansal, G.; Zhang, J.; Wu, Y.; Zhang, S.; Zhu, E.; Li, B.; Jiang, L.; Zhang, X.; and Wang, C. 2023b. Autogen: Enabling next-gen llm applications via multi-agent conversation framework. *arXiv preprint arXiv:2308.08155*.

Wu, T.-H.; Lian, L.; Gonzalez, J. E.; Li, B.; and Darrell, T. 2024. Self-correcting llm-controlled diffusion models. In *Proceedings of the IEEE/CVF Conference on Computer Vision and Pattern Recognition*, 6327–6336.

Yang, D.; Hu, L.; Tian, Y.; Li, Z.; Kelly, C.; Yang, B.; Yang, C.; and Zou, Y. 2024a. WorldGPT: a Sora-inspired video AI agent as Rich world models from text and image inputs. *arXiv preprint arXiv:2403.07944*.

Yang, L.; Yu, Z.; Meng, C.; Xu, M.; Ermon, S.; and Cui, B. 2024b. Mastering Text-to-Image Diffusion: Recapitulating, Planning, and Generating with Multimodal LLMs. *arXiv:2401.11708*.

Yuan, Z.; Chen, R.; Li, Z.; Jia, H.; He, L.; Wang, C.; and Sun, L. 2024. Mora: Enabling generalist video generation via a multi-agent framework. *arXiv preprint arXiv:2403.13248*.

Zhang, L.; Rao, A.; and Agrawala, M. 2023. Adding Conditional Control to Text-to-Image Diffusion Models. *arXiv:2302.05543*.

## Full Prompts for Planning

We present our complete LLM planning prompts in Fig. 6, including 2D layout planning, 3D depth planning, orientation planning, and camera view planning. We fully take advantage of ICL and CoT prompting technique to enhance LLM’s reasoning and decision-making capabilities.

## T2I-3DisBench Benchmark

Owing to the absence of a suitable textual dataset involving multiple objects with various orientations, 3D spatial relationships, and camera views, we construct our own benchmark, namely T2I-3DisBench (3D image scene Benchmark). The benchmark construction process begins with the careful crafting of 10 such complex and detailed prompts. To expand the dataset, we leveraged Claude AI<sup>1</sup> to imitate and generate remaining 40 similar texts, which are subsequently refined by human experts to ensure quality, diversity and consistency. Fig. 7 presents some representative examples in our T2I-3DisBench textual dataset. For evaluation metrics, we find that traditional metrics such as CLIPScore (Radford et al. 2021) or BLIP-CLIP (Li et al. 2022) lacked the necessary precision to capture nuanced details like object orientations or camera views, and the metrics of T2I-compBench (Huang et al. 2023) are inadequate and inaccurate for assessing detailed 3D features. Hence, we employ InternVL (Chen et al. 2024b), a Vision Large Language Model (VLLM), to score the generated images across four dimensions: object count, object orientation, 3D spatial relationship, and camera view. We feed InternVL with the following instruction:

Text: \_\_.

*How well does the image match the text? You need to consider (1) object count, (2) object orientation, (3) 3D spatial relationship between objects, (4) camera view. Return a tuple ("score", X.XXXX), with a float number between 0 and 1. The higher value represents higher text-image alignment.*

<sup>1</sup><https://www.anthropic.com/claude>

With such a versatile instruction, we are able to comprehensively evaluate how well the generated images align with the text in terms of complex 3D details.

- a coffee table is in front of a sofa, a vase is on the left side of the coffee table, three apples next to each other on the center of the table, a table lamp is on the right side of the coffee table, and two roses are in the vase, living room, left view, photorealistic
- a coffee table is in front of a sofa, a vase is on the left side of the coffee table, three apples next to each other on the center of the table, a table lamp is on the right side of the coffee table, and two roses are in the vase, living room, right view, photorealistic
- a coffee table is in front of a sofa, a vase is on the left side of the coffee table, three apples next to each other on the center of the table, a table lamp is on the right side of the coffee table, and two roses are in the vase, living room, front view, photorealistic
- a coffee table is in front of a sofa, a vase is on the left side of the coffee table, three apples next to each other on the center of the table, a table lamp is on the right side of the coffee table, and two roses are in the vase, living room, top view, photorealistic
- bedroom, top view, a bed on top right, a wooden nightstand next to bed with a lamp on it, some flowers on carpet besides bed, a sofa on bottom left with some cushions, a coffee table near the sofa with a vase and a book on it, plane figure, photorealistic
- front view, one vase on the left has two sunflowers facing left, another one vase on the right has one sunflower facing right, three butterflies flying above and facing upwards, in the universe, stars in the distance, photorealistic
- front view, sixteen sheep are lined up in two horizontal rows, first row of eight are facing backward and standing in front, second row of eight are facing forward and standing behind, in the snowing fields, icy, blizzard, photorealistic
- on the left side of room, a toy train facing right is behind three building blocks stacked vertically, on the right side of room, a toy airplane facing left is behind a toy tree, in the toy room, close-ups, camera shooting from the right, photorealistic
- on the left side of room, a toy train facing right is behind three building blocks stacked vertically, on the right side of room, a toy airplane facing left is behind a toy tree, in the toy room, close-ups, camera shooting from the left, photorealistic
- on the left side of room, a toy train facing right is behind three building blocks stacked vertically, on the right side of room, a toy airplane facing left is behind a toy tree, in the toy room, close-ups, camera shooting from the front, photorealistic
- on the left side of room, a toy train facing right is behind three building blocks stacked vertically, on the right side of room, a toy airplane facing left is behind a toy tree, in the toy room, close-ups, camera shooting from the top, photorealistic

Figure 7: **Representative Examples of Prompts in T2I-3DisBench.** Underlines indicate 3D spatial relationships, italics indicate object orientation, blue font indicates the camera view, and gray font indicates the number of objects.

## Implementation details in Blender

In this section, we provide a comprehensive overview of the procedures and code used to assemble 3D objects into a complete 3D scene and render it into a 2D image using Blender (Community 2018). First, we need to initialize a Blender bpy environment, configuring global scene settings and rendering settings. Then, we need to configure the camera parameters according to the planned 3D layout. Subsequently, we import all the 3D objects into the environment and set their corresponding parameters based on the planned 3D layout. Finally, we render the 3D scene into a 2D image, and transform it into a depth map and edge map, which are later leveraged for fine-grained control in the ControlNet (Zhang, Rao, and Agrawala 2023). Our codes are all imple-

mented on the version 4.0.0 of python Blender bpy.

## Environment Initialization

To render a 3D scene into an image, we begin by initializing the Blender environment, setting up both global scene and rendering parameters. For global scene settings, we set background to a low-intensity gray (RGB: 0.1, 0.1, 0.1) using a shader node, creating a consistent gray backdrop. A global light source is positioned at (0, -5, 10) directly above the front of the object for uniform lighting across experiments. For rendering settings, the Blender Cycles rendering engine is used for high-fidelity image output. Depth pass (*use\_pass\_z*) is enabled to extract depth information during rendering, and the color depth is set to 16-bit for better quality. The output resolution is configured to 1024x1024 pixels. The rendered image is saved as a PNG file in the specified directory. Our complete codes are shown in the following.

```
1 # Global Scene Settings
2 world = bpy.data.worlds['World']
3 world.use_nodes = True
4 bg_node = world.node_tree.nodes.get('Background')
5 if bg_node is None:
6     bg_node =
7         world.node_tree.nodes.new('ShaderNodeBackground')
8 bg_node.inputs[0].default_value = (0.1, 0.1, 0.1, 1)
9 bg_node.inputs[1].default_value = 1.0
10 light = bpy.data.objects['Light']
11 light.location = (0, -5, 10)
12 light.rotation_euler = (0, 0, 0)
13 # Rendering Settings
14 scene.render.engine = 'CYCLES'
15 scene.view_layers[0].use_pass_z = True
16 scene.render.image_settings.color_depth = '16'
17 scene.render.resolution_x = 1024
18 scene.render.resolution_y = 1024
19 scene.use_nodes = True
20 scene.render.filepath = os.path.join(output_img_dir,
    "rendering.png")
21 scene.render.image_settings.file_format = 'PNG'
```

## Camera Configuration

After initialize the environment, we configure the camera parameters according to the 3D layout planned by our layout manager. The parameters of camera include the camera position and orientation, corresponding to *location* and *rotation\_euler* in bpy, respectively. We need to translate the camera view in the 3D layout into a parameterized form that Blender understands. For example, the camera position parameter (x,y,z) for “top view” is set to (0,1,15). Our full conversion rules are implemented as follows:

```
1 camera = bpy.data.objects['Camera']
2 if camera_view == "left view":
3     randon_x = random.randint(-10, -5)
4 elif camera_view == "right view":
5     randon_x = random.randint(5, 10)
6 else:
7     randon_x = random.randint(-1, 1)
8 if camera_view == "top view":
9     camera.location = (0, 1, 15)
10 else:
```

```
11     camera.location = (randon_x, -math.sqrt(225 -
    randon_x**2), 5)
12 camera.rotation_euler =
    (math.atan(math.sqrt(camera_x**2 + camera_y**2)
    / (camera_z + 1e-5)), 0, -math.atan(camera_x /
    (camera_y + 1e-5)))
```

## Object Parameter Settings

Next, we import all the 3D objects (OBJ files) into our environment using the *bpy.ops.wm.obj\_import(filepath = " )* function. For each 3D model, we set key parameters, including object size, position, and orientation, which correspond to the *dimensions*, *delta\_location*, and *rotation\_euler* attributes in bpy, respectively. The complete code for our comprehensive conversion process is provided below:

```
1 # Load JSON of 3D Layout
2 with open('3D_layout_info.json', 'r') as file:
3     layout = json.load(file)
4 # Load JSON of Alignment Imformation
5 with open('3D_Model_Aligner_info.json', 'r') as file:
6     align = json.load(file)
7 # Import i-th OBJ File
8 bpy.ops.wm.obj_import(filepath=obj_files[i])
9 # Merge Extra Components
10 if (len(bpy.data.objects) > 3 + i):
11     obs = bpy.context.scene.objects[2:]
12     ctx = bpy.context.copy()
13     ctx['selected_objects'] = obs
14     bpy.ops.object.join()
15 obj = bpy.context.selected_objects[0]
16 # Set 'dimensions'
17 height_width = obj.dimensions[2] / obj.dimensions[0]
18 height_depth = obj.dimensions[2] / obj.dimensions[1]
19 width_depth = obj.dimensions[0] / obj.dimensions[1]
20 max_obj_size = max(obj.dimensions[0],
    obj.dimensions[2])
21 max_item_size = max(layout[i]['width'],
    layout[i]['height'])*10 + layout[i]['depth']
22 if max_obj_size == obj.dimensions[0]:
23     obj.dimensions = (max_item_size, max_item_size /
    width_depth, max_item_size * height_width)
24 else:
25     obj.dimensions = (max_item_size / height_width,
    max_item_size / height_depth, max_item_size)
26 bpy.ops.object.transform_apply(location=False,
    rotation=False, scale=True)
27 bpy.context.view_layer.update()
28 if item_data[i]['depth'] < 0.5:
29     while sum(obj.dimensions) > 25:
30         obj.dimensions = obj.dimensions / 1.5
31         bpy.context.view_layer.update()
32 # Set 'delta_location'
33 bpy.ops.object.origin_set(type='ORIGIN_CENTER_OF_MASS',
    center='BOUNDS')
34 obj.location = (0, 0, 0)
35 obj.delta_location[0] = (layout[i]['left'] +
    layout[i]['width']/2 - 0.5) * 10 * (0.9 +
    layout[i]['depth'])
36 obj.delta_location[1] =
    (layout[i]['depth']-0.1)*(10+obj.dimensions[1])
37 obj.delta_location[2] = -(layout[i]['top'] +
    layout[i]['height']/2 - 0.5) * 10 * (0.9 +
    layout[i]['depth']) - 3 * layout[i]['depth']
```

```

38 bpy.ops.object.transform_apply(location=True,
    rotation=False, scale=False)
39 bpy.context.view_layer.update()
40 # Set 'rotation_euler'
41 rotation = {"forward": [0, 0, 0], "backward": [0, 0,
    math.pi], "left": [0, 0, -90/180 * math.pi],
    "right": [0, 0, 90/180 * math.pi], "upward":
    [-90/180 * math.pi, 0, 0], "downward": [90/
    180 * math.pi, 0, 0]}
42 obj.rotation_euler = [x+y for x, y in zip(aligned[i],
    rotation[layout[i]['orientation']])]
43 bpy.ops.object.transform_apply(location=False,
    rotation=True, scale=False)
44 bpy.context.view_layer.update()

```

These conversion rules ensure accurate translation of the planned 3D layout into Blender’s 3D simulation environment, referencing the face-camera-view orientation of object as determined by the 3D model engineer. Through such comprehensive parameter configurations, we achieve high alignment of object placement with the planned 3D layout.

## Image Rendering

After setting all the parameters, we now successfully assemble the 3D scene. We are able to render the complete 3D scene into a 2D image with accuracy using the `bpy.ops.render.render(True)` function. This 2D rendering is further transformed into both a depth map and an edge map, which are used for fine-grained control in the ControlNet (Zhang, Rao, and Agrawala 2023). To generate the depth map, we use a depth node within Blender to capture the Z-depth values of the 3D objects. This depth information is crucial for understanding the spatial relationships between objects in the scene. For the edge map, we employ OpenCV to detect the contours in the rendered image. This edge map highlights the boundaries and shapes of objects, providing additional information that aids in the precise control and manipulation of the 3D scene. Our specific codes are presented in the following.

```

1 # Depth Map
2 tree = scene.node_tree
3 links = tree.links
4 # Clear Nodes
5 for n in tree.nodes:
6     tree.nodes.remove(n)
7 render_layers_node =
8     tree.nodes.new(type='CompositorNodeRLayers')
9 invert_node =
10     tree.nodes.new(type='CompositorNodeInvert')
11 depth_output_node =
12     tree.nodes.new(type='CompositorNodeOutputFile')
13 depth_output_node.base_path = output_img_dir +
14     "/depth"
15 depth_output_node.file_slots[0].path = "depth000"
16 map_node = tree.nodes.new('CompositorNodeMapValue')
17 map_node.offset = [-20]
18 map_node.size = [0.1]
19 links.new(render_layers_node.outputs[2],
20     map_node.inputs[0])
21 links.new(map_node.outputs[0], invert_node.inputs[1])
22 links.new(invert_node.outputs[0],
23     depth_output_node.inputs[0])

```

```

18 # Rendering Image
19 bpy.ops.render.render(write_still=True)
20 # Edge Map
21 import cv2
22 image = cv2.imread(os.path.join(output_img_dir,
23     "rendering.png"))
24 edges = cv2.Canny(image, 100, 200)
25 cv2.imwrite(os.path.join(output_img_dir,
26     "canny_edges.png"), edges)

```

The meticulous setup of the environment, precise configuration of camera parameters and object parameters collectively contribute to high-quality rendering. This high-quality rendering is essential for effectively controlling the 3D properties of the generated image. As a result, it facilitates our precise and reliable 3D-controllable image generation.

## Ablation of ControlNet Parameters

We conduct comparative experiments with different control scales and inference steps of ControlNets to determine the optimal parameter settings. The *controlscale* parameter ranges from 0.1 to 0.9, and the *inferencesteps* parameter ranges from 5 to 25. As shown in Fig. 8, we select several representative parameter values and visualize the comparison results. The results indicate that increasing the control scale enhances the alignment of the generated images with the input condition images. However, this improvement comes at the cost of reduced image quality. To balance these effects, the optimal control scale parameter is identified as 0.5. For inference steps, the quality of the generated images improves with an increasing number of steps. However, once the number of steps exceeds 20, the image quality gains plateau. Therefore, 20 inference steps are chosen as the optimal inference parameter in our experimental setup.

## More Qualitative Comparisons

Figure 9 and Figure 10 present more qualitative comparisons between our MUSES and existing state-of-the-art methods, including both open-source models and commercial API products, such as Stable Diffusion V3 (Esser et al. 2024), DALL-E 3 (Betker et al. 2023), and Midjourney v6.0 (Midjourney 2024). Obviously, our systematic collaborative approach generates images that are more faithful to the details of the text, in terms of object count, orientation, 3D spatial relationships, and camera view. Additionally, when dealing with such complex and detailed prompts, our system incorporates a human verification step following the 2D-to-3D Layout Manager’s initial planning. This human-in-the-loop approach further ensures that the planned layout reasonably represents the details in the user input. It also demonstrates the potential for human-AI collaboration in tackling such complex visual generation tasks.



### ICL Prompt of 2D Layout Planning:

You are a master of image layout planning.

Your **task** is to plan the realistic layout of the image according to the given prompt. The generated layout must follow the CSS style, where each line starts with the object description and is followed by its absolute position.

Formally, each line should be like "*object* *{{width: ?px; height: ?px; left: ?px; top: ?px; }}*", with each object extracted from the given prompt. The image is 256px wide and 256px high. Therefore, all properties of the positions must not exceed 256px, including the addition of left and width and the addition of top and height.

Some examples are given below.

Example 1: {}

Example 2: {}

Example 3: {}

Example 4: {}

Example 5: {}

User Input: {}

Layout Information:

### CoT Prompt of 3D Depth Planning:

**\*\*User Input:** {}

**\*\*Layout Information:** {}

Your **task** is to determine the depth value (greater than 0 and less than 1) for each object contained in the layout information based on the user input. Actually, depth value represents the distance of the object from the viewer. **First**, carefully look for the words among “back”, “behind”, “front” and “hidden” in the user input. If not found, directly set all depth values to “0.0”. If find one, go to the **second** step with the following setting **rules**:

- If “Object1 in front of Object2”, the depth value of Object1 is smaller and can be “0.1” and the depth value of Object2 can be “0.9”.
- If “Object1 behind (hidden by) Object2”, the depth value of Object1 is bigger and can be “0.9” and the depth value of Object2 can be “0.1”.
- If “Object in the back”, the depth value of Object is big and can be “0.9”.
- If “Object in the front”, the depth value of Object is small and can be “0.1”.

Your final answer must be a list of tuples as [(object name, depth), ...], where object name is the same as layout information. Follow the above two steps and give some explanation. Do not include any code.

### CoT Prompt of 3D Orientation Planning:

**\*\*User Input:** {}

**\*\*Layout Information:** {}

Your **task** is to determine the orientation value for each object contained in the layout information based on the user input. **First**, carefully look for the words among “facing”, “towards” and “heading” in the user input. If not found, directly set all orientation values to “forward”. If find one, go to the **second** step with the following setting **rule**:

- Extract the directions among “forward”, “backward”, “left”, “right”, “upward” and “downward” from the user input as the orientation values.

Your final answer must be a list of tuples as [(object name, orientation), ...], where object name is the same as layout information. Follow the above two steps and give some explanation. Do not include any code.

### CoT Prompt of 3DCamera View Planning:

**\*\*User Input:** {}

Your **task** is to extract the camera view from the user input. First, carefully look for the word “view” in the user input. If not found, directly set the camera view to “front view”. If find one, go to the second step with the following setting **rule**:

- Extract strings among “front view”, “left view”, “right view” or “top view” from the user input as the camera view.

Your final answer must be in JSON format, where key is “camera view” and value is one of the strings “front view”, “left view”, “right view” or “top view”. Follow the above two steps and give some explanation. Do not include any code.

Figure 6: **Full Planning Prompts in our 2D-to-3D Layout Manager.** There are four planning prompts in total, including ICL 2D layout planning, CoT 3D depth planning, CoT orientation planning, and CoT camera view planning.

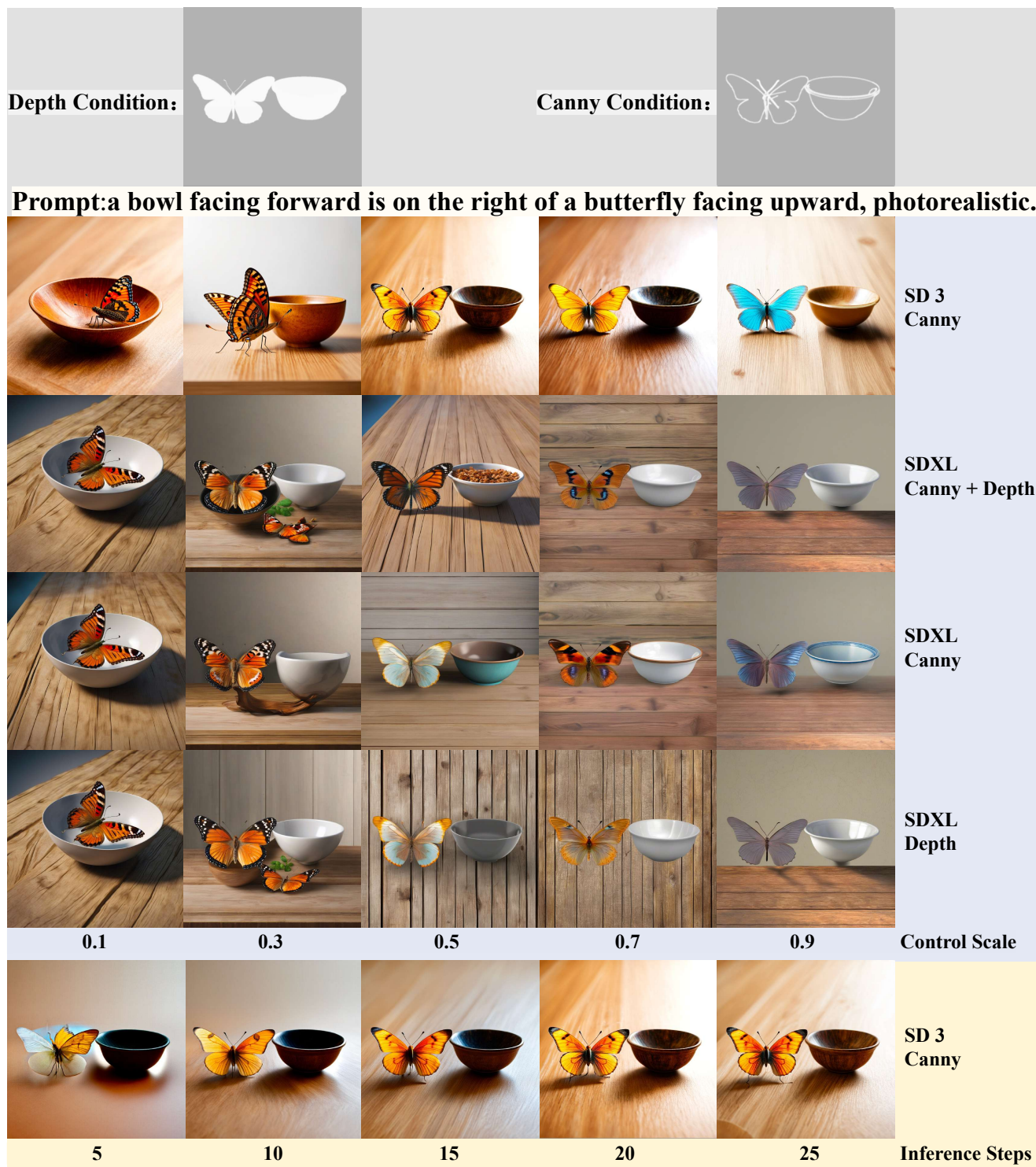


Figure 8: **Qualitative Comparison with Different Inference Steps and Control Scale Parameters of ControlNets.** The larger the control scale, the higher the alignment of the generated image with the input conditions, but the lower the image fidelity. Meanwhile, as the inference steps increase, the image quality improves until it is saturated (after 20 inference steps).





one teddy bear is facing left, another teddy bear is facing right, the two are sitting on the white carpet surrounded by three toy cars, facing left, forward and right, respectively, at the space station, captured from the front, lighting from the right, photorealistic

on the bottom half of the image, twenty cars driving from the left to the right on a path, in smoggy weather with fog, top view; on the top half of the image, desert background, with dust storms in the distance, photorealistic

grassy field at sunset, front view, a large tree stump in the center, a smiling little girl sitting on the stump and facing right, a cat on the left facing right, a dog on the right facing left, orange-yellow sky in the distance, masterpiece, oil painting style

three airplanes flying in the air, facing left, forward and right, respectively, an eagle flying underneath the center airplane, a boy facing right standing on the left, a girl facing left standing on the right, a beautiful path stretching into the distance, colorful, anime style

cozy bedroom, top view, a bed on the top right, a wooden nightstand next to the bed with a lamp on it, some flowers on the carpet besides the bed, a sofa on the bottom left with some cushions, a coffee table near the sofa with a vase and a book on it, a plane figure, best quality, photorealistic

four old trains are lined up on parallel railway tracks, each painted in vibrant colors, with billowing steam, foggy weather, green land background, 4K resolution, best quality, masterpiece, top view, photorealistic

a park bench facing forward is in the center, a dog facing left is next to the bench on the right, a bicycle facing left is leaning against a tree facing forward on the left, children playing in the background grass, in the park, front view, photorealistic

Figure 9: **Qualitative Comparison (1) With Existing SOTA Methods.** Our MUSES consistently demonstrates the highest text-image alignment, regarding object count, object orientation, 3D spatial relationship between objects, and camera view. We compare our MUSES with SOTA open-sourced models and closed-sourced commercial API products, including Stable Diffusion V3, Hunyuan-Dit, Playground v2.5, DALL-E 3, and Midjourney v6.0. Color-marked texts on the far right represent important 3D details.



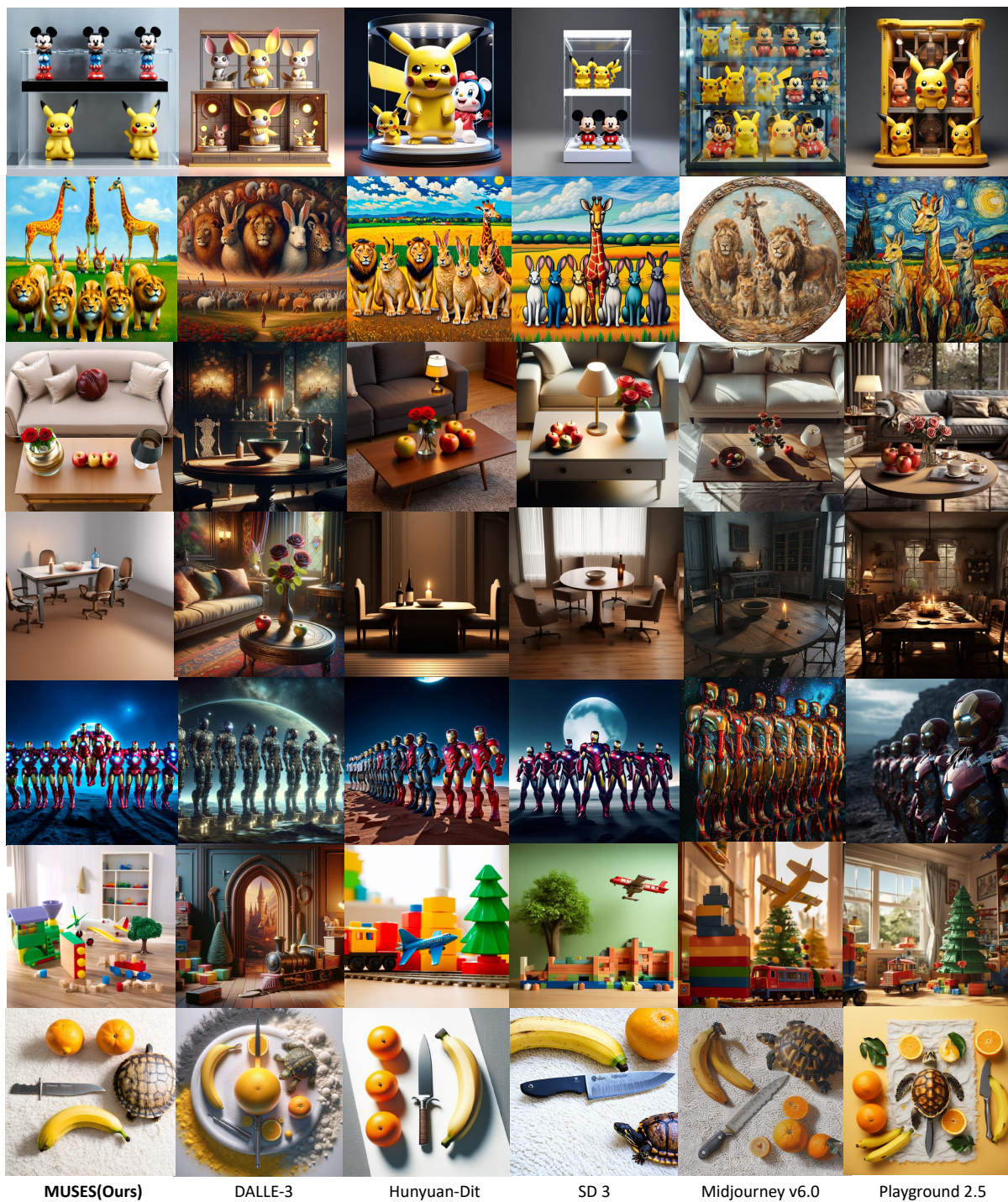


Figure 10: **Qualitative Comparison (2) With Existing SOTA Methods.** Our MUSES consistently demonstrates the highest text-image alignment, regarding object count, object orientation, 3D spatial relationship between objects, and camera view. We compare our MUSES with SOTA open-sourced models and closed-sourced commercial API products, including Stable Diffusion V3, Hunyuan-Dit, Playground v2.5, DALL-E 3, and Midjourney v6.0. **Color-marked texts** on the far right represent important 3D details.